Nonlinear Laser-Plasma Interaction in Magnetized Liner Inertial Fusion

Matthias Geissel[a], T.J. Awe[a], D.E. Bliss[a], M.E. Campbell[b], M.R. Gomez[a], E. Harding[a], A.J. Harvey-Thompson[a], S.B. Hansen[a], C. Jennings[a], M.W. Kimmel[a], P. Knapp[a], S.M. Lewis[c], R.D. McBride[a], K. Peterson[a], M. Schollmeier[a], D.J. Scoglietti[a], A.B. Sefkow[a], J.E. Shores[a], D.B. Sinars[a], S.A.Slutz[a], I.C. Smith[a], C.S. Speas[a], R.A. Vesey[a], and J.L. Porter[a]

[a]Sandia National Laboratories, Albuquerque, New Mexico
[b]Laboratory for Laser Energetics, Rochester, New York
[c]University of Texas, Austin, Texas

ABSTRACT

Sandia National Laboratories is pursuing a variation of Magneto-Inertial Fusion called Magnetized Liner Inertial Fusion, or MagLIF. The MagLIF approach requires magnetization of the deuterium fuel, which is accomplished by an initial external B-Field and laser-driven pre-heat. While magnetization is crucial to the concept, it is challenging to couple sufficient energy to the fuel, since laser-plasma instabilities exist, and a compromise between laser spot size, laser entrance window thickness, and fuel density must be found. Nonlinear processes in laser plasma interaction, or laser-plasma instabilities (LPI), complicate the deposition of laser energy by enhanced absorption, backscatter, filamentation and beam-spray. Key LPI processes are determined, and mitigation methods are discussed. Results with and without improvement measures are presented.

Keywords: MagLIF, LPI, laser plasma interaction, SBS, high energy lasers

1. INTRODUCTION

Magnetized Liner Inertial Fusion (MagLIF) is an approach for thermonuclear fusion that is driven by Sandia's Z Pulsed Power Facility. More than 20 MA of drive current are channeled into a centimeter-sized deuterium filled beryllium liner. The resulting magnetic pressure implodes the liner and compresses the fuel therein. Since the involved time scales in the electric discharge and compression are too long to adiabatically heat cold fuel to fusion temperatures due to involved cooling rates, magnetization is used as a method to increase the temperature and reduce heat losses.[1] A dedicated, smaller pulsed power device is feeding electromagnetic coils and fired prior to the main Z discharge.[2] This creates an axial magnetic field of about 10 T inside the liner, parallel to its axis. Shortly after Z fires, when the liner is barely starting to implode, the Z-Beamlet laser[3] is delivering 2-4 kJ of laser light at 526.6 nm through a polyimide window into the fuel, creating a plasma with temperatures of several 100 eV. Since the charged particles of the plasma cannot freely move across field lines of the previously applied axial magnetic field (and vice versa), the magnetic field gets compressed and amplified once the liner implodes. This strong axial magnetic field forces electrons to spiral along the axis, which greatly reduces heat losses that would normally occur due to electron conduction. Early MagLIF experiments demonstrated that neutron yields increased dramatically if an initial B-field was applied and the fuel was pre-heated with Z-Beamlet. Either of these processes by themselves did not accomplish such an enhancement.[4] However, even these encouraging results fell dramatically short of the predictions from 1-D simulations. Plasma diagnostic results and more elaborate 2-D simulations suggested that only 200-300 J out of the 2 kJ laser pulse were coupled to the fuel. The balance was either absorbed near the window or back-scattered/reflected. Consequently, the study and control of the pre-heat process became a priority effort of the program concentrating on fuel densities between 1.5% and 5% of the critical electron density ($4 \times 10^{21} cm^{-3}$). Average laser intensities were between 40 and 300 TW/cm^2, but local peak intensities can exceed the average by factors of 2-4 in hot spots.

2. LASER-PLASMA INTERACTION

Heating gaseous fuel is predominately accomplished by inverse bremsstrahlung, which is a well understood process. The absorption increases with density and decreases with temperature. If laser target interaction were purely based on inverse bremsstrahlung, just a few hundred joules of laser energy would cause the Laser-Entrance-Hole window (LEH) to become transparent. However, it was experimentally observed that even a $1\,\mu$m thin polyester window can block a $2\,$kJ laser pulse. This fact is mostly rooted in the presence of laser plasma instabilities (LPI), which are caused by laser driven electrostatic waves in a plasma: If an intense laser beam propagates through a plasma, electrons oscillate in the electric field of the light with the plasma-frequency, which is below the laser frequency. Since oscillating charges are emitting electromagnetic radiation in turn, the result is a superposition of waves that creates a beat mode. The ponderomotive force finally expels electrons from the high intensity regions of the beat mode into low-intensity regions. Figure 1 shows a simplified sketch of this process. This resonant process forms a repetitive density modulation in the medium, similar to a volume grating, which can interact with the laser beam and drive instabilities. All instabilities develop essentially following an exponential growth function in space:

$$E_{LPI} \propto e^{\kappa\ell}, \tag{1}$$

where E_{LPI} is the energy invested into laser plasma instabilities, κ is the linear growth coefficient for LPI, and ℓ is the interaction path length in the plasma. κ grows linear with laser intensity I_{las} and with the ratio between electron density and critical density n_e/n_{crit}. The following subsections introduce the various nonlinear processes.

2.1 Stimulated Brillouin Scattering

A familiar process of scattering light waves on density modulations is Stimulated Brillouin Scattering (SBS).[5,6] This phenomenon is also observed in large optics or long fibers, and it is a primary damage concern for CW fiber lasers. In a plasma, laser photons can couple into an ion acoustic wave, which is the charge carrying equivalent of a sound wave. Since the ions have significant mass, the energy transfer from photon to ion is low, and the scattered wave experiences only a small change in wavelength (less than 1%). SBS is strong for long pulses, since the build-up is dependent on ion-acoustic time scales of many picoseconds. Multi-nanosecond pulses can experience dramatic SBS coupling.

2.2 Stimulated Raman Scattering

In a plasma, the term Stimulated Raman Scattering (SRS) relates to a different process than what Raman scattering originally refers to.[7] Both processes, however, are inelastic. While the classical Raman effect leads

a) – laser wave initiating particle oscillation   b) – beat mode driving electrons to low–field regions.
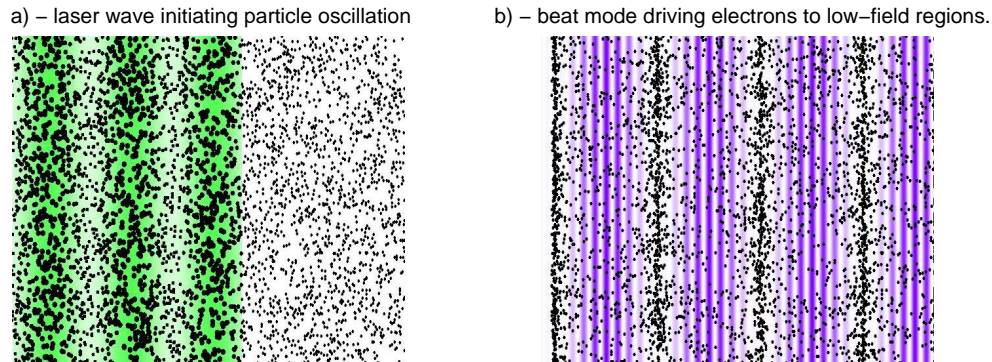

Figure 1. Simplified sketch of the process that leads to electrostatic waves. A laser wave entering from the left forces electrons to oscillate in its E-field (a: The electron "dot-size" represents the spatial depth relative to the image plane). The oscillating electrons emit radiation at a sightly longer wavelength, combining with the original wave to a beat-mode (b). The ponderomotive force in the high-field areas of the beat mode forces electrons into low-field areas, leading to a repetitive density modulation. Laser light can interact with this "volume-grating-like" structure and scatter or be absorbed.

to an energy transfer from light to vibrational (and sometimes rotational) states of molecules, SRS in a plasma happens when photons couple to an electron-plasma wave, also called a plasmon. Energy transfer to the low-mass electrons can be significant and lead to large red-shifts of the wavelength of the scattered light (up to a factor of two). For many experiments, the capacity of SRS to produce hot electrons is a big concern. Time scales for SRS are defined by the electron oscillation frequency, an optical time scale which is substantially below a picosecond and therefore practically instantaneous for nanosecond laser heating processes.

2.3 Two Plasmon Decay

Closely related to SRS is the Two Plasmon Decay (TPD).[8] This phenomenon can be understood through the relation between electron density and laser frequency:

$$\frac{\omega_{las}^2}{\omega_p^2} = \frac{n_{crit}}{n_e}, \tag{2}$$

where ω_{las}, ω_p are the frequencies of the laser and the plasma oscillation, and n_e, n_{crit} are the electron density in the plasma and the critical density associated with the laser wavelength. When the plasma density is exactly a quarter of the critical density, each laser photon carries exactly twice the energy of a plasmon. Hence it is possible that the photon is expended to create two plasmons. TPD is a dominant concern for hot electron generation. Since the plasma densities for MagLIF are currently below $0.25 \times n_{crit}$, TPD is not a concern for heating the fuel. However, it can occur during the destruction phase of the LEH.

2.4 Filamentation

While not being a cause of enhanced backscatter or absorption it itself, the process of filamentation or self-focusing can increase LPI and deflect laser propagation. Since LPI increases exponentially, a local enhancement of laser intensity can dramatically increase LPI.[6] If the spatial profile of the laser illumination shows strong modulations, or 'hot spots', the increased electric field and temperature in the hot spots cause electrons to migrate into cooler areas due to conduction and ponderomotive force. This creates a gradient of electron density that increases the refractive index N in the hot spots, as we can understand from the relation between electron density and refractive index:

$$N^2 = (1 - \frac{n_e}{n_{crit}}) \tag{3}$$

In effect, each hot spot creates a micro-lens, further increasing the laser intensity. In addition, a more extended gradient of plasma density can lead to a larger slope of the refractive index, which can cause a refractive change of the filament's direction. A random mix of such slopes can then lead to an effective beam spray that enlarges the beam size far beyond the original envelope. It becomes obvious, that a well controlled intensity distribution is essential. Filamentation occurs on a hydrodynamic time scale, which is similar but slightly slower than ion acoustic time scales. Table 1 shows a synopsis of nonlinear processes in a plasma.

Table 1. Synopsis of dominant nonlinear processes in laser-palsma interaction.

	SBS	SRS	TPD	Filamentation
Coupling mech.	ion acoustic wave	electron plasma wave	electron plasma wave	density gradient(s)
Wavelength shift	< 1%	up to 2x	(annihilated)	none
Relevant time scale	acoustic	optical	optical	hydrodynamic
Primary concern	backscatter	backscatter, absorption	absorption	beam spray, LPI amplification

3. LPI MITIGATION CONCEPTS

To minimize LPI build-up, one can change the laser intensity or the electron density. Because LPI actually scales with the ratio between electron density and laser-specific critical density n_{crit}, it is also very beneficial to use lasers with shorter wavelength, which influences n_{crit} by a square dependance (see also Eq. 2). In many cases, such as at Sandia, the laser wavelength is a constant for practical and budgetary reasons. The density can be varied, but in the case of MagLIF this affects the achievable gain because the total volume of fuel changes. More practical is a change in focus size, and even more important is the definition and smoothness of the laser's intensity distribution on target. Since a relatively large focus is desirable, one may want to defocus the laser to the anticipated ideal spot size. Without additional optical elements, this leads to an ill-defined intensity distribution caused by an "intermediate" imaging plane, which is neither the relay-imaged near field of the collimated beam nor its far field Fourier equivalent, the plane of best focus. Defocused near-flat-top beams of high energy lasers, which lack a perfect Gaussian cross-section, are prone to very strong modulations and irregular hot-spot distributions. As described in Sec. 2.4, such modulations will lead to filamentation and subsequently amplify the LPI build-up. Consequently, just defocusing a beam is not a valid method to reduce LPI. A better solution is to control the spot size in the focal plane by using random phase plates[9] or their better defined successors, the distributed phase plates.[10, 11] These optical elements effectively scramble the phase front information and project laser light to a pre-defined area. Local phase front and intensity variations are averaged over the whole illuminated area. In this process, rays from wide ranging areas of the phase plate interfere in the focal plane and cause interference speckles which also exhibit a deep modulation. Fortunately, heat conduction in a plasma acts fast enough over the small scale of a speckle to reduce temperature gradient driven filamentation. A comparison of measured laser spots with and without phase plate is shown in Fig. 2. If conduction does not suffice to suppress LPI, Smoothing by Spectral Dispersion (SSD[12]) can be applied. In SSD, a dispersive element introduces slight angle variations for each wavelength that is present in the spectrum of the laser. When focused, the laser spot is slightly displaced for different wavelength, which leads to a smoothing in the dispersive plane if the bandwidth of the laser is sufficiently large (typically 10s or 100s of GHz). Beyond this, additional measures such as 2-dimensional SSD, Polarization Smoothing,[13] or Induced Spatial Incoherence (ISI[14]) can be used for further LPI mitigation. Currently, Z-Beamlet has not sufficient bandwidth to efficiently apply SSD. The beam profile for MagLFIF pre-heat experiments therefore relies on LPI mitigation through an appropriate choice of phase plate.
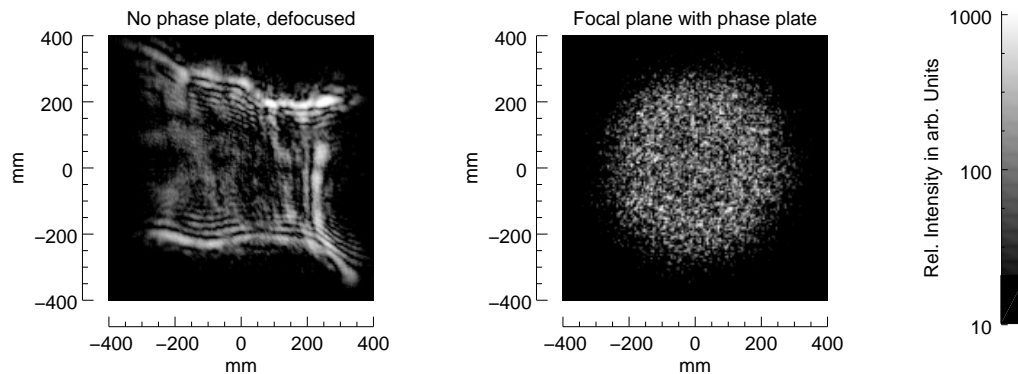

Figure 2. Comparison of laser illumination without a phase plate and defocused (left) and a similar sized illumination with a 750 μm phase plate at best focus. The images are scaled logarithmically to enhance lower intensity features of the spot without phase plate. The high intensity areas in the unconditioned beam (without phase plate) can cause filamentation and LPI amplification.

4. LPI MEASUREMENTS

LPI can either be measured indirectly by comparing pre-heat performance such as LEH penetration or laser penetration into the gas and assuming that improvements are attributed to reduced LPI, or one can directly measure the signature byproducts of LPI, such as backscattered radiation or hot electrons. Since hot electrons in a highly magnetized gas are widely confined and high-Z tracer layers change the cooling rate and laser propagation into the fuel, MagLIF experiments are better suited to employ backscatter measurements. We define two areas of backscatter: First, there is intra-beam backscatter, which is light that travels directly back towards the laser. Based on the volume-diffractive nature of SBS and SRS, the scattered light is phase-conjugated and intra-beam scattering represents a large fraction of total backscatter. However, the backscattered light can spread significantly beyond the original envelope of the beam if filamentation occurs. In this case Near-Beam-Imaging (NBI) comes into play, the second backscatter area. At Sandia, NBI has been measured by mounting reflective panels close to the final optics elements inside of the target chamber of Z as sketched in Fig. 3a. Filtered camera recordings capture intensity and size of the backscattered light. Intra-beam measurements were performed by placing a target-facing fiber into the soft edge of the laser beam (also indicated in Fig. 3a). The light that is captured by this fiber is analyzed by a streaked spectrometer. The pre-heat measurements shown in this article were done without firing Z itself. All experiments used a 500 ps pre-pulse to decompress the window, aiding in better laser penetration overall.
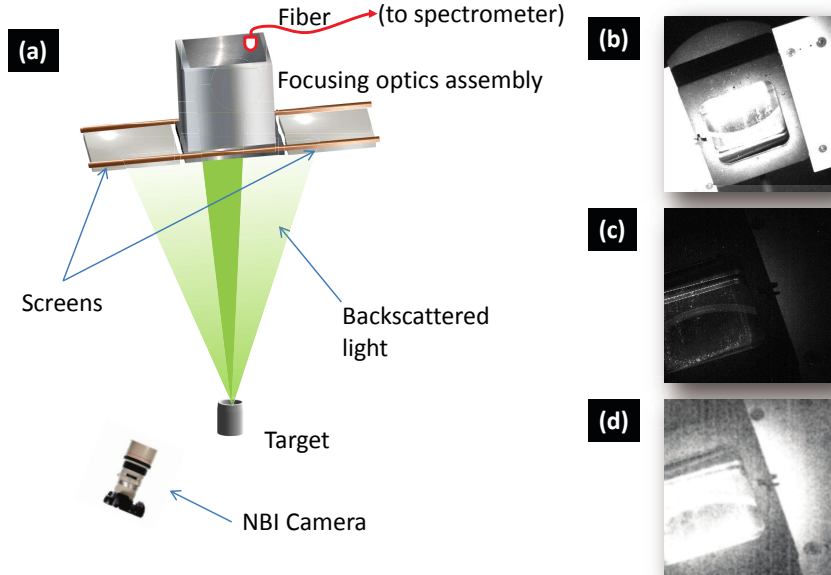

Figure 3. Illustration of the Near-Beam-Imaging system in Z: (a) - a sketch of the mounted NBI screens relative to laser beam and target with intra-beam fiber. The target was exposed to a 9.5 T magnetic field parallel to the cylinder axis (B-Field coils not shown). (b) - an image of SBS for a shot without phase plate. (c) - an image of a shot with phase plate. (d) - worst case brightness correction for the image with phase plate.

Unfortunately, the camera setup for the first campaign got destroyed by electromagnetic pulse during shots soon after the experiment. The replacement was not identical in field-of-view and sensitivity, complicating direct comparisons. Image processing was performed to match the vacuum window's brightness. This is a worst case scenario, since this brightness is either determined by scatter from the incoming "downstream" laser light, which is roughly identical for both shots, or by the "upstream" backscattered light, which will be less with phase plate and therefore overestimates the recorded backscatter. This assumption holds true as long as the phase plate does not increase backscatter, which was confirmed with the intra-beam measurement. Figure 3b shows the image for a shot into 60 psi deuterium without phase plate. The approximate, defocused spot size on the LEH was 600-650 μm. Image c) shows the result with phase plate and new camera setup for an identical target

configuration. Even if brightened up to worst case, the total brightness on the screens and the scatter radius are much smaller than without phase plate. The spot diameter created by the phase plate was measured to $650\,\mu$m (FWHM). The main laser pulse delivered roughly $2\,$kJ in a $2\,$ns main pulse, whcih rose to 50% of the maximum intensity at $2.5\,$ns after the peak of the pre-pulse.

The intra-beam measurements clearly show a reduction in SBS. Figure 4 shows a $4\,$kJ shot with $1.8\,$mm phase plate versus a $2\,$kJ shot with $700\,\mu$m unconditioned beam. The large and smooth beam leads to a small fraction of SBS in spite of the much higher laser energy. More refined measurements are underway in a dedicated target chamber. The $2\,$kJ shot had the same temporal pulse form as the experiments described in Fig. 3. The $4\,$kJ shot used a $3.5\,$ns main pulse that rose to 50% of the main intensity at $1.5\,$ns after the peak of the pre-pulse.
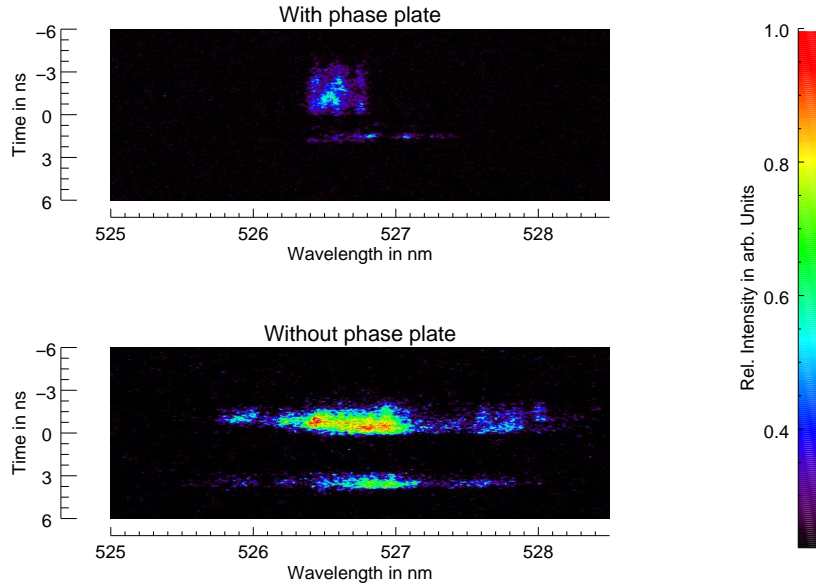

Figure 4. Comparison of a $4\,$kJ shot with a large phase plate (top) and a $2\,$kJ shot with unconditioned beam at roughly $700\,\mu$m diameter (bottom). Despite the higher energy, there is a dramatic reduction of SBS for the case with a large diameter phase plate.

4.1 Influence of LPI on LEH transmission

A comparison of LEH transmission with and without phase plate clearly demonstrates the benefit of a smoother, conditioned beam. Table 2 shows the results for two transmission measurements through a $1\,\mu$m polyester foil with a $10\,$mm defocused beam (the spot size is about $1\,$mm) and with a large phase plate of $2\,$mm FWHM, where the "maximum" is chosen to be the average intensity of the speckled center region of the focus rather than the highest speckle intensity. Even though the much smaller spot would heat the foil much more easily and therefore penetrate better in the absence of LPI, the large and conditioned beam shows 40% more laser penetration. Transmission measurements were done without applied B-Field by using a whole-beam calorimeter behind the target. Since beam spray into solid angles beyond the coverage of the calorimeter is possible, these values represent lower boundaries for the actual transmission.

Table 2. Comparison of window penetration with and without phase plate.

Shot-#	Phase Plate	Spot Size	Laser energy	Transmission
B14060203	No	$1\,$mm	$4000\,$J	38%
B14090903	Yes	$2\,$mm	$4014\,$J	53%

5. SUMMARY AND OUTLOOK

Laser penetration through dense plasmas is subject to complex resonant processes. Filamentation and the build-up of electrostatic waves in the plasma can lead to strong nonlinear effects, such as SBS, SRS, and TPD. These processes can enhance absorption and backscatter, leading to reduced laser heating in the plasma depths of interest for MagLIF. LPI can be measured, and the effect can be minimized by applying smooth beam profiles, preferably with distributed phase plates. While more precise measurements are on the way, the benefit of suitable phase plates for MagLIF was already demonstrated at Sandia National Laboratories. The MagLIF program is now in the progress to optimize laser intensity for the pre-heat phase of the experiments with dedicated phase plates. Experiments in collaboration with Lawrence Livermore National Laboratories in California at the National Ignition Facility and with the University of Rochester at the Laboratory of Laser Energetics in New York will investigate the benefit of using SSD or 3ω frequency conversion. These results will help to increase the detailed understanding of the relevant processes to optimize the performance of MagLIF experiments.

ACKNOWLEDGMENTS

REFERENCES

1. S.A. Slutz, M.C. Herrmann, R.A. Vesey, A.B. Sefkow, et al.: Phys. Plasmas **17**, 056303 (2010)
2. D.C. Rovang, D.C. Lamppa, M.E. Cuneo, A.C. Owen, et al.: Rev. Sci. Instrum. **85**, 124701 (2014)
3. Patrick K. Rambo, Ian C. Smith, John L. Porter, et al.: Appl. Optics **44**(12), 2421 (2005)
4. M.R. Gomez, S.A. Slutz, A.B. Sefkow, et al.: Phys. Rev. Lett. **113**, 155003 (2014)
5. C. Labaune, E. Fabre, A. Michard, and F. Briand: Phys. Rev. A **32**, 577 (1985)
6. D.H. Froula, L. Divol, N.B. Meezan, S. Dixit, et al.: Phys. Rev. Lett. **98**, 085001 (2007)
7. R.P. Drake, R.E. Turner, B.F. Lasinski, et al.: Phys. Fluids **31**(10), 3130 (1988)
8. H. Figueroa, H. Joshi, H. Azechi, et al.: Phys. Fluids **27**(7), 1887 (1984)
9. Y. Kato, K. Mima, N. Miyanaga, et al.: Phys. Rev. Lett. **53**, 1057 (1984)
10. S.N. Dixit, J.K. Lawson, K.R. Manes, H.T. Powell, and K.A. Nugent: Opt. Lett. **19**(6), 417 (1994)
11. Y. Lin, T.J. Kessler, and G.N. Lawrence: Opt. Lett. **20**(7), 764 (1995)
12. S. Skupsky, R.W. Short, T. Kessler, et al.: J. Appl. Phys. **86**(8), 3456 (1989)
13. K. Tsubakimoto, M. Nakatsuka, H. Nakano, et al.: Opt. Commun. **91**, 9 (1992)
14. R.H. Lehmberg, A.J. Schmitt, and S.E. Bodner: J. Appl. Phys. **62**, 2680 (1987)